Preprints, 10th IFAC International Symposium on
Advanced Control of Chemical Processes
Shenyang, Liaoning, China, July 25-27, 2018

Application of Economics Optimizing Control to a Two-step Transesterification Reaction in a Pilot-Scale Reactive Distillation Column

Daniel Haßkerl[*], Clemens Lindscheid[*], Sankaranarayanan Subramanian[*], Steven Markert[*], Andrzej Górak[**], Sebastian Engell[*]

[*] *Process Dynamics and Operations Group, TU Dortmund University, 44221 Dortmund Germany,*
[**] *Laboratory of Fluid Separations, TU Dortmund University, 44221 Dortmund Germany,*
(Tel.: +49-231-755-3419; E-mail:{Daniel.Hasskerl, Clemens.Lindscheid, Sankaranarayanan.Subramanian, Steven.Markert, Andrzej.Gorak, Sebastian.Engell}@tu-dortmund.de).

Abstract: The challenges in the chemical process industry of tighter environmental and safety constraints, a higher economic efficiency and an operation in a more dynamic environment motivate the utilization of optimizing control where economic policies are integrated into a (often nonlinear) model predictive control scheme. This so-called one-layer approach or dynamic real-time optimization (D-RTO) has the advantage that the processes are dynamically steered towards the most profitable region. High-fidelity dynamic process models are a basic prerequisite for a good controller performance, and building such models is a challenge. Using highly complex models also may lead to long computation times and thus feedback delays. These issues are in practice avoided by applying only steady-state optimization based on nonlinear models (RTO) and/or using simplified models in MPC. However, the development of computational methods that are able to solve large-scale dynamic optimization problems efficiently have paved the way for applications of economics optimizing control to complex chemical processes. In this contribution, we will demonstrate that a real complex pilot-scale chemical processes, a two-step transesterification realized by reactive distillation that is described by a large DAE model can be operated at the economic optimum by using direct optimizing control. We discuss the problem formulation and the numerical methods used and show experimental data that were obtained at the real process.

Keywords: Economics optimizing control, Extended Kalman Filter, Nonlinear DAE-systems, Reactive distillation.

1. INTRODUCTION

For economic performance optimization, classically a two-layer approach is employed where a steady state optimization is combined with a model predictive controller (MPC) which has the objective to track the optimal set-points that were computed by steady state optimization. Usually, the MPC controllers are based on linear process models that were parameterized from plant experiments. Such MPC controllers can include an economic steady-state optimization that is cast in the form or an LP problem. In economics optimizing MPC, the plant economics are improved directly by optimizing an economic or economically motivated cost function over the prediction horizon in the nonlinear model predictive control (NMPC) formulation, also called one-layer approach or dynamic real-time optimization (D-RTO) (Engell, 2007). The main advantage of this approach compared to the classical two layer approach is the integrated dynamic and steady-state optimization of the process based on a single process model.

Since its invention in the 1970s in the petrochemical industry, linear MPC gained ground in many industrial sectors such as the chemical, mechanical, aerospace and automotive industry with more than 9,500 applications in 2005 (Dittmar and Pfeiffer, 2006). For the nonlinear counterpart of MPC, much fewer applications to real processes can be found due to various reasons, see e.g. (Foss and Schei, 2007). Among those reasons are the costs, the time and the need for specialized staff that are associated with the development of a process model that can describe the dynamic and steady state process behavior with the required accuracy, the lack of efficient optimization techniques for solving the resulting large nonlinear and non-concave optimization problems as well as robustness and stability issues. Due to these challenges, applications of NMPC in general and of economic optimizing NMPC in particular have been rare, despite its high potential to improve the performance of any chemical process, see e.g. the study of the economics optimizing control approach for a similar case study (Idris and Engell, 2011, 2012).

In this contribution, we discuss the prototypical application of an NMPC scheme with economic cost function to a real complex intensified chemical process. The implementation is

[1] The research leading to these results has received funding from the European Commission under the grant agreement number 291458 (ERC Advanced Investigator Grant MOBOCON).

supported by efficient software tools such as automatic differentiation (AD) and the interior-point optimizer Ipopt (Wächter and Biegler, 2006). Automatic differentiation is used for the efficient generation of first and second order derivative information. The Hessian and the Jacobians that are computed by AD are used in Ipopt to solve the resulting large nonlinear optimization problems efficiently. The optimizing controller makes use of a high-fidelity dynamic nonlinear process model to ensure a good controller performance. We apply economics optimizing NMPC to optimize the operation of a pilot-scale reactive distillation (RD) process in which the homogeneously-catalyzed two-step transesterification reaction of dimethyl carbonate (DMC) with ethanol (EtOH) is realized. This chemical process has industrial relevance and is able to produce two valuable products, the intermediate product ethyl methyl carbonate (EMC) and the final product diethyl carbonate (DEC). The two products are obtained both at the bottom of the column and by shifting the operational conditions in the reactive distillation column either of the two products can be obtained at a high purity. We will focus here on the results that were obtained for the production of the product diethyl carbonate.

The paper is structured as follows: In section 2, we start with a description of the chemical process, the sensing technology and the automation of the plant. The NMPC formulation and its software realization are described in section 3. The realization at the pilot-scale plant is presented in section 4 and the results that were obtained are shown in section 5. Conclusions and an outlook on future work follow in section 6.

2. CHEMICAL PROCESS AND PROCESS MODEL

2.1 Process description

The homogeneously catalyzed transesterification of dimethyl carbonate (DMC) with ethanol (EtOH) in a reactive distillation process is described in detail in (Keller et al., 2012) and (Keller 2013). Sodium ethoxide catalyzes the synthesis of ethyl methyl carbonate (EMC) and of diethyl carbonate (DEC) from DMC and EtOH in two consecutive equilibrium-limited reaction steps. The catalyst is diluted in the EtOH feed because it tends to precipitate in carbonate-rich solutions. In order to prevent the catalyst from precipitating, both reactants and the catalyst solution are fed using a single liquid distributor at a packing height of 2 m. The homogeneously catalyzed transesterification reaction takes place at and below the feed position (in the stripping section). According to their boiling points, the products (EMC and DEC) are concentrated in the bottom product stream while the distillate stream consists of alcohols and DMC. The process has four degrees of freedom that can be used to steer the operation of the plant, the feed flowrate of DMC ($Feed_{DMC}$) which is related to the flowrate of EtOH to realize a total flowrate of 4 [kg/h], the amount of the catalyst that is diluted in the EtOH feed relative to the overall feed flow rate (x_{cat}), the reflux ratio (RR) and the distillate-to-feed-ratio (DF), see Fig. 1.

The setpoint of the distillate-to-feed ratio is tracked by the control system of the process by manipulating the boil-up rate. The remaining parameters such as the setpoints of the feed and reflux temperature as well as the overall feed flowrate were fixed to the values given in (Keller et al., 2012).

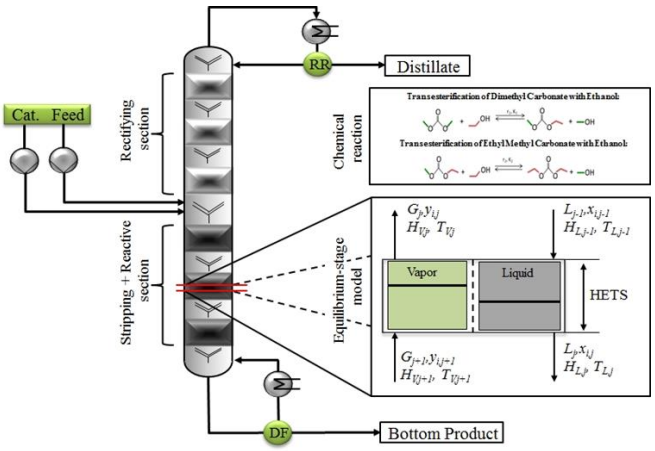

Figure 1: Schematic view of the reactive distillation process with its degrees of freedom

2.2 Process hardware and process automation

The pilot-scale reactive distillation column that was used in the experimental work is made of glass, has a diameter of 50 mm and can be operated at or below ambient pressure. The active column height consists of six structured packing sections of Sulzer BX^{TM} packing material with an overall packing height of 5.4 m. Compared to the experimental setup shown in (Keller et al., 2012), some modifications were made. The natural circulation reboiler was replaced by a direct evaporator (Normag AG) with a maximum volume of 2.2 l and a total heat duty of 3 kW in order to reduce the time needed for the start-up and for the shutdown procedures. The compositions of bottom and distillate streams are determined on-line using near-infrared spectroscopy (NIR) (ABB/ Thermo Fischer Inc.). The concentration profile along the packing is measured off-line by analyzing samples that were taken along the column using a gas chromatograph (GC). The column is fully automated using a Siemens PCS7 control system. For the data exchange between the control system and the direct optimizing controller, an OPC DA (Open Platform Communications Data Access) server is used.

2.3 Process model

In (Keller 2013), several mathematical models were presented for the pilot-scale process that all are based on the MESH (Material, Equilibrium, Summation, Enthalpy or Heat balance) equations. From the set of models presented in (Keller 2013), the EQ-Kin (equilibrium-stage model using reaction kinetics) model was selected (cf. Fig. 1) for the state estimation and the control task. This model is a compromise between sufficient accuracy and complexity. The column model incorporates equations for each column element i.e. for the condenser, the reboiler, the liquid distributors and the active packing. The packing model is based on an equilibrium stage model which contains the molar balance equations for each stage

$$\frac{dx_{i,j} \cdot N_{tot,j}}{dt} = \sum_{l}^{n_{in}} F_{l,i,j} - \sum_{k}^{n_{out}} F_{k,i,j} + \sum_{r=1}^{n_r} r_{r,j}, \quad (1)$$

where at each stage $j = 1, \dots, n_j$, n_{in} inflows and n_{out} outflows of each component i ($i \in \{MeOH, EtOH, DMC, EMC, DEC\}$, number of components $n_c = 5$) are considered. HETP values were assumed as constant and equal to 0.2 m. The summation condition gives $\sum_{i=1}^{n_c} x_{i,j} = \sum_{i=1}^{n_c} y_{i,j} = 1$, $j = 1, \dots, n_j$. The vapor and liquid phase composition is assumed to be in equilibrium. The vapor-liquid equilibrium is computed from the extended Raoult's law i.e. $y_{i,j} = K_{i,j}^{VLE} \cdot x_{i,j}$, with the vapor-liquid equilibrium constant for each component i of stage j, $K_{i,j}^{VLE} = \frac{\gamma_i(x_{i,j}, T_j) \cdot p_{0i,j}^{LV}(T_j)}{P_j}$ that requires the computation of the activity coefficients (a UNIQUAC model is used to compute the activity coefficients γ_i). The correlations for the saturated pressure $p_{0i,j}^{LV}$ were taken from (Keller 2013). The reaction kinetics $r_{r,j}$ result from the activity-based model of the two-step ($n_r = 2$) chemical reaction. The mathematical formulation of the model of the reactive distillation column using the MESH equations results in a set of 186 differential and 288 algebraic equations. Libraries for the correlations of the physical properties, the equilibrium calculations, hold-up and pressure drop correlations complete the model equations (see (Keller 2013) for further details on the underlying MESH model).
The mathematical model can be represented as a general discrete-time DAE system as follows:

$$\begin{aligned} x_k &= f(x_{k-1}, z_{k-1}, u_{k-1}) \\ 0 &= g(x_k, z_k, u_{k-1}) \\ y_k &= h(x_k, z_k), \end{aligned} \quad (2)$$

where $x_k \in \mathbb{R}^{n_x}$ and $z_k \in \mathbb{R}^{n_z}$ refer to the differential and algebraic states, $y_k \in \mathbb{R}^m$ represents the measurements and $u_k \in \mathbb{R}^{n_u}$ represents the control input at each sampling instant k. $f: \mathbb{R}^{n_x} \times \mathbb{R}^{n_z} \times \mathbb{R}^{n_u} \to \mathbb{R}^{n_x}$ and $g: \mathbb{R}^{n_x} \times \mathbb{R}^{n_z} \times \mathbb{R}^{n_u} \to \mathbb{R}^{n_z}$ denote the differential and algebraic equations and $h: \mathbb{R}^{n_x} \times \mathbb{R}^{n_z} \to \mathbb{R}^{n_y}$ is the measurement function that includes measurements from the set of differential and algebraic state variables. Among the numerous measurements that are available at the pilot-plant, 19 measurements were used for process control, see Tab. 1.

Table 1: Measurements at the RD column that are used for the state estimator

Name	Measured state	Packing height
Condenser	Liquid Composition	above 5.4m
Liquid Distributor 1	Vapor temperature	5.4m
Liquid Distributor 2	Vapor temperature	4.2m
Liquid Distributor 3	Vapor temperature	3.0m
Liquid Distributor 4	Vapor temperature	1.0m
Liquid Distributor 5	Vapor temperature	0.5m
Liquid Distributor 6	Vapor temperature	0.0m
Reboiler	Liquid temperature, Liquid composition, Liquid holdup	Below the packing

3. ECONOMICS OPTIMIZING CONTROL

With the increase of computational power and the development of efficient optimization algorithms, economics optimizing or D-RTO schemes which are based on rigorous dynamic nonlinear models have become feasible.

3.1 General control problem

The optimization problem of the nominal NMPC that is based on a Lagrangian-type cost function with the associated stage cost $J(\boldsymbol{s}_{k+1}, \boldsymbol{u}_k)$ for equal prediction and control horizons of n_k steps can be formulated as

$$\min_{\boldsymbol{u}_k, \boldsymbol{s}_0, \boldsymbol{s}_{k+1} \forall k \in \{0, \dots, n_k - 1\}} J(\boldsymbol{s}_{k+1}, \boldsymbol{u}_k) = \sum_{k=0}^{n_k - 1} L(\boldsymbol{s}_{k+1}, \boldsymbol{u}_k)$$

$$\begin{aligned} \text{subject to} \quad \boldsymbol{s}_{k+1} &= \boldsymbol{F}(\boldsymbol{s}_k, \boldsymbol{u}_k, \boldsymbol{p}) && \forall k \in \{0, \dots, n_k - 1\}, \\ 0 &= \boldsymbol{G}(\boldsymbol{s}_{k+1}, \boldsymbol{u}_k, \boldsymbol{p}) && \forall k \in \{0, \dots, n_k - 1\}, \\ \boldsymbol{s}_{lb} &\le \boldsymbol{s}_k \le \boldsymbol{s}_{ub} && \forall k \in \{0, \dots, n_k\}, \\ \boldsymbol{u}_{lb} &\le \boldsymbol{u}_k \le \boldsymbol{u}_{ub} && \forall k \in \{0, \dots, n_k - 1\}, \\ \boldsymbol{g}_{lb} &\le \boldsymbol{g}(\boldsymbol{s}_{k+1}, \boldsymbol{u}_k) \le \boldsymbol{g}_{ub} && \forall k \in \{0, \dots, n_k - 1\}. \end{aligned} \quad (3)$$

where $\boldsymbol{p} \in \mathbb{R}^{n_p}$ are model parameters and $\boldsymbol{u}_k \in \mathbb{R}^{n_u}$ are piecewise constant inputs. The elements of the state vector $\boldsymbol{s}_k = [\boldsymbol{x}_k, \boldsymbol{z}_k] \in \mathbb{R}^{n_x + n_z}$ which contains the differential states $\boldsymbol{x}_k$ and the algebraic states $\boldsymbol{z}_k$ are also NLP variables which are constrained by dynamic and algebraic equations $\boldsymbol{F}(\cdot): \mathbb{R}^{n_x} \times \mathbb{R}^{n_z} \times \mathbb{R}^{n_u} \times \mathbb{R}^{n_p} \to \mathbb{R}^{n_x}$ and $\boldsymbol{G}(\cdot): \mathbb{R}^{n_x} \times \mathbb{R}^{n_z} \times \mathbb{R}^{n_u} \times \mathbb{R}^{n_p} \to \mathbb{R}^{n_z}$. $\boldsymbol{g}(\boldsymbol{s}_{k+1}, \boldsymbol{u}_k)$ represents the possibly nonlinear equality and inequality constraint functions besides constraints on the inputs. If the constraints are satisfied, the solution to the above problem is the optimal state and input trajectory $\forall k \in \{0, \dots, n_k - 1\}$ (denoted by *)

$$(\boldsymbol{s}_0^*, \boldsymbol{s}_{k+1}^*, \boldsymbol{u}_k^*) = \underset{\boldsymbol{u}_k, \boldsymbol{s}_0, \boldsymbol{s}_{k+1} \forall k \in \{0, \dots, n_k - 1\}}{arg\,\min} J(\boldsymbol{s}_{k+1}, \boldsymbol{u}_k) \quad (4)$$

of which only the inputs $\boldsymbol{u}_0^*$ of the first interval are applied and then the optimization is iterated with new information.

3.2 Tailored control problem for reactive distillation

In many chemical processes, the product stream should be maximized but the product can be sold at a reasonable price only if it has a required purity. Thus the purity requirement constitutes a constraint to the optimal control problem. Implementing this constraint as a hard constraint however may lead to an infeasible problem (even if only formulated as a terminal constraint) because it may not be possible to meet it in transient situations. Therefore we propose to add the purity requirement to the soft constraint function $\boldsymbol{g}_{soft}(\boldsymbol{s}_{k+1}, \boldsymbol{u}_k, \boldsymbol{\varepsilon}_{k+1})$ that is realized as an additional contribution to the stage cost. The final dynamic control problem (5) has three contributions, the maximization of revenue minus the associated costs, the regularization of the inputs using the weighting matrix $\boldsymbol{Q}_u$ in order to avoid frequent input moves and the contributions realized by the soft constraints. The final dynamic optimal control problem

that implements direct optimizing control on a finite horizon including all aspects discussed so far reads as

$$\min_{\boldsymbol{u}_k, \boldsymbol{s}_0, \boldsymbol{s}_{k+1}, \boldsymbol{\varepsilon}_{k+1} \forall k \in \{0,\dots,n_k-1\}} J_{D-RTO}(\boldsymbol{s}_{k+1}, \boldsymbol{u}_k, \boldsymbol{\varepsilon}_{k+1}) =$$
$$\alpha_e \left(\sum_{k=0}^{n_k-1} -Pr_{DEC}\left(x_{k+1,DEC,B_k}\right) \cdot \dot{B}_k + \sum_{f=1}^{n_u} C_f \cdot u_{k,f} \right) + \alpha_t \sum_{k=0}^{n_k-1} \left(\sum_{f=1}^{n_u} \Delta u_{k,f}^T \cdot \boldsymbol{Q}_u^{-1} \cdot \Delta u_{k,f} \right)$$
$$+ \sum_{k=0}^{n_k-1} \sum_{i=1}^{n_{soft}} \alpha_i \cdot \boldsymbol{\varepsilon}_{k+1,i}{}^2$$

subject to

$$\begin{aligned}
\boldsymbol{s}_{k+1} &= \boldsymbol{F}(\boldsymbol{s}_k, \boldsymbol{u}_k, \boldsymbol{p}) && \forall k \in \{0,\dots,n_k-1\},\\
0 &= \boldsymbol{G}(\boldsymbol{s}_{k+1}, \boldsymbol{u}_k, \boldsymbol{p}) && \forall k \in \{0,\dots,n_k-1\},\\
\boldsymbol{s}_{lb} &\le \boldsymbol{s}_k \le \boldsymbol{s}_{ub} && \forall k \in \{0,\dots,n_k\},\\
\boldsymbol{u}_{lb} &\le \boldsymbol{u}_k \le \boldsymbol{u}_{ub} && \forall k \in \{0,\dots,n_k-1\},\\
\boldsymbol{g}_{soft,lb} &\le \boldsymbol{g}_{soft}(\boldsymbol{s}_{k+1}, \boldsymbol{u}_k, \boldsymbol{\varepsilon}_{k+1}) \le \boldsymbol{g}_{soft,ub} && \forall k \in \{0,\dots,n_k-1\},\\
\boldsymbol{g}_{lb} &\le \boldsymbol{g}(\boldsymbol{s}_{k+1}, \boldsymbol{u}_k) \le \boldsymbol{g}_{ub} && \forall k \in \{0,\dots,n_k-1\},\\
0 &\le \boldsymbol{\varepsilon}_{k+1} && \forall k \in \{0,\dots,n_k-1\}.
\end{aligned} \tag{5}$$

The initial state which is required for the solution of the control problem is estimated using an Extended Kalman Filter (EKF) for Differential Algebraic Equations (DAE) as described in (Purohit et al., 2013). Note that by using the problem formulation (5), we can easily fix the initial state $\boldsymbol{s}_0$ by replacing the corresponding bounds $\boldsymbol{s}_{lb}, \boldsymbol{s}_{ub}$ with the most recent vector of (consistent) estimates. As the measurements of the composition have a sampling time of 40 seconds compared to the major sampling frequency of 10 seconds of the other measurements (see Table 1), we used a multi-rate formulation with a fixed structure for the DAE-EKF.

3.3 Software realization

The software tool *do-mpc* (Lucia et al., 2014 and Lucia et al., 2017) is an off-the-shelf implementation for NMPC written in the Python programming language and was used as a starting point for the implementation of economics optimizing control. *do-mpc* makes use of CasADi (Andersson et al., 2012a, 2012b) to realize automatic differentiation of the symbolic representation of the process model for efficient computations of the first and second derivative information and has an interface to the interior-point optimizer Ipopt. *do-mpc* has a modular structure consisting of the receding-horizon optimal control problem, a template for the state estimator, a simulator and the model and problem formulation. It supports fast NMPC developments and facilitates the application to real processes by replacing the simulator with the real process. We exploited the modular structure of the implementation further by parallelizing the modules and by defining a common interface for an efficient data exchange between the individual modules.

Table 2: Parametrization of the optimizing controller

Controller	Parameter values
Prediction horizon, *np*	5
Control Horizon, *nk*	5
Sampling time, *Δt*	10 [min]
Finite elements	1
Order of the Lagrange polynomial	1
Collocation grid	Radau
Optimizer	Ipopt
Hessian/ Jacobian	exact
Linear solver	MA27

Four modules are defined for four different tasks (see below), parallelized by multithreading and run on separate CPUs using a timer each (the sampling times of each module used in this work are parenthesized).

1. *Simulator module* (not used in the application to the real plant, only used for real-time simulation studies): the module cyclically takes the provided inputs, numerically integrates the state variables using the routine *idas* (Hindmarsh et al., 2005) over the sampling instance and writes the states and measurements to the server. State and measurement noise with a given standard deviation can be added by setting the respective flag.
2. *Estimator module*: At every sampling instance (sampling time of 10 seconds) of the estimator, the module reads the current measurements and process inputs from the OPC server, executes a single estimation step (here by using a DAE-EKF) and writes the estimates and estimated output to the OPC server.
3. *Optimizer module*: At every sampling instance (sampling time of 10 minutes) of the optimizer, the module takes the estimates that were computed most recently and updates the initial point of the optimization problem with process feedback. The optimization problem is *solved until convergence* and if the optimization routine successfully finished the optimization, the first set of optimal controls are written to the OPC server.
4. *Visualization module*: At every sampling instance (sampling time of 30 seconds), this module collects the measurements, inputs, estimates and estimated output from the different modules and plots the data over a predefined window into the past in time-graphs.

4. REALIZATION AT THE PILOT-SCLAE PLANT

The overall structure of the economics optimizing controller implementation is shown in Fig. 2. Using this structure, we can easily switch between a real-time simulation for testing purposes or the application to the RD process by rewiring the OPC server connection in the local network.

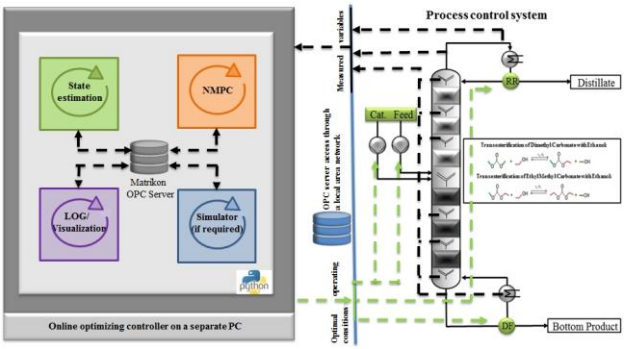

Figure 2: Local network and connections of the modules of the automation framework for the RD case study

4. RESULTS

In total six experiments at six different days were conducted at the RD column by enabling the optimizing controller in a steady state condition after the manual start-up of the process. Five experiments (E1-E5) were carried out in which a minimum required purity of the final product DEC of

0.25 [mol/mol] should be reached so that the process is considered to operate profitably. In a sixth experiment (E6), the minimum required purity of the product DEC in the bottom product stream was set to a value of 0.4 [mol/mol]. The price for the product DEC of 21.29 [€/kg] as well as the costs for the reactants (EtOH: 1.78 [€/kg], DMC: 1.95 [€/kg]) and the utilities (catalyst: 100.0 [€/kg] and energy demand that is associated with the distillate-to-feed ratio and the reflux ratio: 4.25×10^{-3} [€/W]) were assumed to be constant for all six experiments. At the beginning of each experiment, the holdup of the column was filled with the alcohol EtOH and heated up to the boiling point while a feed flowrate of 3.5 [kg/h] EtOH and 0.5 [kg/h] DMC was realized before the optimizing controller was started.

4.1 Performance of the controller

Fig. 3 displays the estimates of the DAE-EKF and the measurements of the temperatures and concentration profiles along the packing during the first two hours of the experiment E3 in which the production of DEC is established. It can be seen that the estimated profiles using the online temperature measurements and the online near-infrared spectroscopy (NIR) in the top and bottom stream are in good agreement with the manually sampled data using the gas chromatography (GC). Only at the initial point, larger deviations are present due to the initialization of the estimation. It can be seen that the state estimator converges to the true plant state within the first hour. Fig. 4 displays the trajectories of the controls and of the composition that was measured in the condenser and in the evaporator. It can be seen that the controller achieved the required purity of DEC quickly by feeding the more expensive reactant DMC and the expensive catalyst, in order to reduce the costs associated with violating the minimum purity constraint. After the minimum purity requirement was reached, the product price contribution in the cost function becomes relevant which leads to a reduction of the amount of catalyst and the adjustment of the molar feed ratio, using more of the cheaper reactant EtOH.

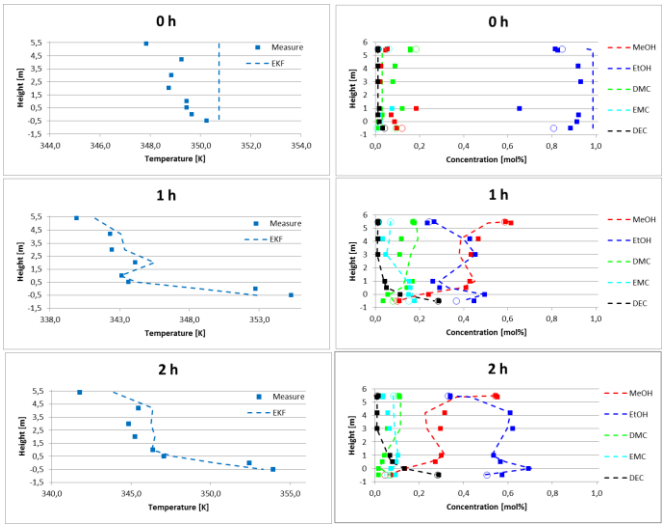

Figure 3: Estimated (‘dashed’ lines) and measured (GC: ‘square’’marks, NIR: ‘circular’ marks) column temperature and concentration profile during the experiment E3.

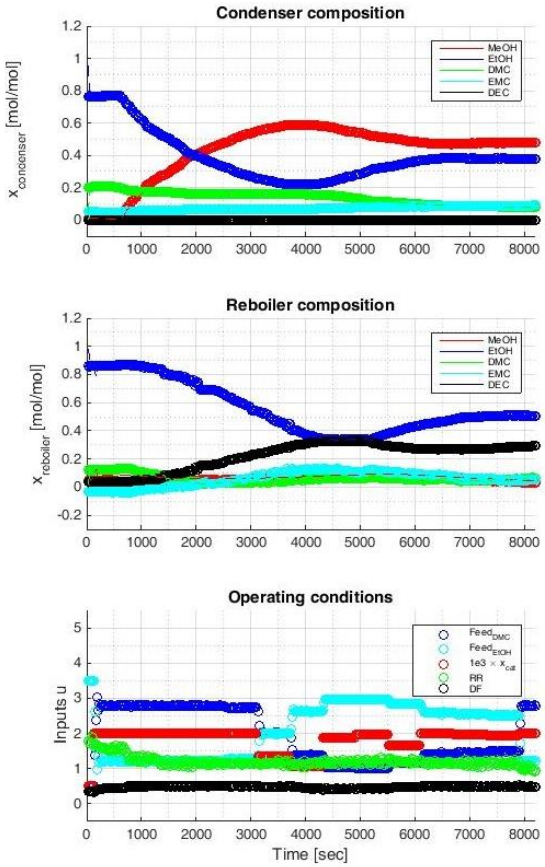

Figure 4: Estimated (‘dashed’ lines) and measured (‘circular’ marks) trajectories of the condenser and reboiler composition as well as the controls that were realized by the optimizing controller during the first two hours of experiment E4.

4.2 Plant economics

The benefit per second for the production of DEC for each of the experiments is diplayed in Fig. 5. It can be seen that for experiments E1-E5, the optimizing controller could steer the process to a very similar profit with an average value of 35,23 [€/h] for a required purity of the product of 0.25 [mol/mol]. If a larger value for the purity is required and as the price for which the product can be sold is not adapted to the higher purity, the benefit drops significantly due to the different process conditions (see E6). To reach the higher purity, more of the expensive reactant DMC is required and a larger value for the boilup had to be realized. This means that the bottom product flowrate decreases and thus, the expenses for the plant operation increase while the production decreases.

4.4 Reproducibility

The experiments E1-E5 were performed on different days, each after a manual start-up of the RD column and each with the same set-up of the direct optimizing controller. For all experiments, the same process behaviour could be observed, which led to a similar steady state. Only in experiment E4, a lower value for profit can be seen due to a lower revenue as a result of a lowered bottom product stream which had a value of 1.96 [kg/h], while the average value was 2.22 [kg/h A

reason for this may be that the activity of the catalyst was lower in expierment E4 and thus the optimizing controller had to adapt the remaining three inputs.

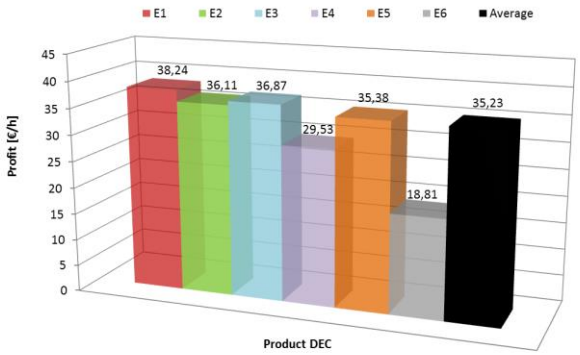

Figure 5: Steady-state plant economics for the experiments E1-E6 determined by using reconciled gas chromatography measurements.

5. CONCLUSIONS

The paper shows the application of economics optimizing control to a challenging real pilot-scale reactive distillation process. The optimizing controller is based on a high-order DAE-model that is necessary to describe such a process reliably and its performance was evaluated by using experiments at the real plant. The computation times were between 4.0 seconds and 18.0 seconds for the optimizer during all the experiments which is a fraction of the sampling time (10 minutes). The multi-rate DAE-EKF that was realized to reconstruct the system state from the measurements at the plant had an average computation time of 0.3 seconds, at a sampling time of 10 seconds. The overall framework that used the *mpi4py* functionality to parallelize the multi-rate state estimation and the optimizing control task using different threads was very efficient so that a large-scale chemical process could be optimized dynamically in real time. Using adaptions of the software tool *do-mpc* for the application, the optimizing controller managed to steer the plant to the production of DEC with a desired purity and to optimize the profitability of the operation of the plant. The controller exhibited an excellent performance during dynamic and steady-state process operation with a conversion of the reactants above 65% at steady state and a selectivity towards the product DEC above 60%. The present work paves the way towards further applications of optimizing control to pilot-scale or industrial-scale processes and provides a suitable software structure for other realizations of NMPC. In future work, we will also address the issue of how to cope with plant-model mismatch, employing multi-stage MPC approach (Lucia et al., 2014).

ACKNOWLEDGEMENTS

The authors gratefully acknowledge inspiring discussions with Dr. Radoslav Paulen, now with the Institute of Information Engineering, Automation and Mathematics in Slovak University of Technology, Bratislava.

REFERENCES

Andersson J., Akesson J., and Diehl M. (2012a), CasADi – A symbolic package for automatic differentiation and optimal control. In Recent Advances in Algorithmic Differentiation, Lecture Notes in Computational Science and Engineering, pp. 297–307

Andersson J., Akesson J., and Diehl M. (2012b), Dynamic optimization with CasADi, Proc. of the 51st IEEE Conference on Decision and Control, pp. 681–686

Dittmar, R., Pfeiffer, B.-M. (2006), Modellbasierte prädiktive Regelung in der industriellen Praxis (Industrial Application of Model Predictive Control), Automatisierungstechnik, 54 (12), pp.590-601

Engell, S. (2007). Feedback control for optimal process operation. Journal of Process Control 17 (3), pp. 203–219

Engell S., Idris E.N.A. (2012), Economics-based NMPC strategies for the operation and control of a continuous catalytic distillation process, Journal of Process Control 22, pp. 1832–1843

Foss, B. A., Schei, T. S. (2007). Putting Nonlinear Model Predictive Control into Use. In R. Findeisen, F. Allgöwer, and L. T. Biegler (Eds.), Lecture Notes in Control and Information Sciences. Assessment and Future Directions of Nonlinear Model Predictive Control 358, pp. 407–417, Springer Verlag, Berlin, Heidelberg

Hindmarsh, A. C., Brown, P. N., Grant, K. E., Lee, S. L., Serban, R., Shumaker, D. E., Woodward, C. S. (2005), SUNDIALS. ACM Transactions on Mathematical Software, 31(3), pp. 363–396

Idris, E., Engell, S. (2011). Real-Time Optimizing Nonlinear Control Applied to a Continuous Reactive Distillation Process. Proc. of the 18th World Congress (IFAC), 44(1), pp. 4892–4897

Keller T., (2013) Reactive distillation for multiple-reaction systems: experimental investigation, modelling and optimisation, Dissertation TU Dortmund, München

Keller T., Holtbruegge J., Górak A., (2012) Transesterification of dimethyl carbonate with ethanol in a pilot-scale reactive distillation column, Chemical Engineering Journal 180, pp. 309–322

Lucia S., Andersson J.A., Brandt H., Diehl M., Engell S., (2014) Handling uncertainty in economic nonlinear model predictive control: A comparative case study, Journal of Process Control 24, pp. 1247–1259

S. Lucia, A. Tatulea-Codrean, C. Schoppmeyer, and S. Engell, (2017) Rapid development of modular and sustainable nonlinear model predictive control solutions. Control Engineering Practice, 60, pp. 51-62

Purohit J.L., Patwardhan S.C., Mahajani S.M., (2013) DAE-EKF-Based Nonlinear Predictive Control of Reactive Distillation Systems Exhibiting Input and Output Multiplicities, Ind. Eng. Chem. Res. 5, pp. 13699–13716

Wächter A., Biegler L.T., (2006) On the implementation of an interior-point filter line-search algorithm for large-scale nonlinear programming, Math. Program. 106, pp. 25–57